



1 **Abstract.** When black carbon (BC) is internally mixed with other atmospheric particles,
2 BC light absorption is effectively enhanced. This study is the first to explicitly resolve
3 the optical properties of coated BC in snow, based on core/shell Mie theory and a snow,
4 ice, and aerosol radiative model (SNICAR). Our results indicate that a ‘BC coating
5 effect’ enhances the reduction of snow albedo by a factor of 1.1–1.8 for a non-absorbing
6 shell and 1.1–1.3 for an absorbing shell, depending on BC concentration, snow grain
7 radius, and core/shell ratio. We develop parameterizations of the BC coating effect for
8 application to climate models, which provides a convenient way to accurately estimate
9 the climate impact of BC in snow. Finally, based on a comprehensive set of in situ
10 measurements across the Northern Hemisphere, we find that the contribution of the BC
11 coating effect to snow light absorption has exceeded that of dust over northern China.
12 Notably, the high enhancements of snow albedo reductions by BC coating effect were
13 found in the Arctic and Tibetan Plateau, suggesting a greater contribution of BC to the
14 retreat of Arctic sea ice and Tibetan glaciers.

15



1 **1 Introduction**

2 Snow is the most reflective natural substance at Earth's surface and covers more
3 than 30% of global land area (Cohen and Rind, 1991). Snow albedo feedback is
4 considered one of the major energy balance factors of the climate system. Previous
5 observations have revealed that light-absorbing particles (LAPs; e.g., black carbon
6 (BC), organic carbon (OC), and mineral dust) within snow can reduce snow albedo and
7 enhance the absorption of solar radiation (Hadley and Kirchstetter, 2012). As a result,
8 LAPs play a significant role in altering snow morphology and snowmelt processes, and
9 therefore have important effects on local hydrological cycles and global climate (Qian
10 et al., 2009).

11 Given the importance of the climate feedback caused by LAPs in snow, studies
12 have developed snow radiative models and sought to improve our understanding of the
13 influence of LAP-contaminated snow on climate. For example, Warren and Wiscombe
14 (1980) developed a radiative forcing model based on Mie theory and δ -Eddington
15 approximation, and reported that snow albedo in visible wavelengths could be reduced
16 by 5%–15% when 1000 ng g⁻¹ BC is present in snow. Flanner et al. (2007) developed
17 a more comprehensive snow albedo model (the snow, ice, and aerosol radiation model;
18 SNICAR) for multilayer snowpack using the two-stream radiative transfer solution. In
19 addition to BC, the SNICAR model also accounts for the potential effects of dust
20 particles and volcanic ash on snow albedo. Recent studies have indicated that snow
21 grain shape also has an important influence on snow albedo (e.g., Dang et al., 2016).



1 Although efforts have been made to optimize snow albedo models, current models
2 still suffer from major limitations. Studies have indicated that when BC in the
3 atmosphere is coated with other aerosols it can significantly enhance light absorption
4 via a lensing effect compared with uncoated BC, as investigated using model
5 simulations (e.g., Jacobson 2001; Matsui et al., 2018) and experimental measurements
6 (e.g., Cappa et al., 2012; Peng et al., 2016). Moreover, coated BC has been observed to
7 exist for only a few hours after emission in some regions (Moteki et al., 2007; Moffet
8 and Prather, 2009). Global aerosol models that simulate microphysical processes have
9 indicated that most BC is mixed with other particles within 1–5 days (Jacobson, 2001)
10 at all altitudes (Aquila et al., 2011). Hence, the climate impacts of BC must be evaluated
11 in the context of the effect of coating on light absorption enhancement.

12 Although the BC coating effect on light absorption enhancement in the atmosphere
13 is broadly acknowledged, little research has been carried out on snow albedo. Flanner
14 et al. (2007) developed the first radiative transfer model to investigate the coating effect
15 on snow albedo, using sulfate as the BC particle coating with a constant absorption
16 enhancement factor of ~1.5. Subsequently, Wang et al. (2017) used a similar constant
17 light absorption enhancement factor for their spectral albedo model for dirty snow
18 (SAMDS). However, the factor varies with the optical properties of different coatings,
19 the core/shell ratio, wavelength, and other parameters in real environments (Lack and
20 Cappa, 2010; Liu et al., 2017). For example, Liu et al. (2017) reported that the core/shell
21 ratio is a key control on light absorption enhancement. You et al. (2016) suggested that



1 light absorption enhancement is highly correlated with visible or near-infrared (NIR)
2 wavelengths and coating material. Furthermore, a core/shell Mie theory simulation
3 (Lack and Cappa, 2010) found light absorption enhancement was smaller for mildly
4 absorbing coatings (e.g., OC) than non-absorbing coatings (e.g., sulfate). Hence, using
5 a constant enhancement factor will result in biased simulation estimates, against
6 refining our knowledge of the hydrological and climate impacts of BC in snow.

7 In this study we apply core/shell Mie theory to calculate the optical properties of
8 BC coated with both mildly absorbing OC and non-absorbing sulfate, and use these
9 results within a SNICAR model to evaluate the influence on snow albedo.
10 Parameterizations for the BC coating effect are then developed for application in other
11 snow albedo and climate models. Finally, we estimate the enhancements of snow albedo
12 reductions and associated radiative forcing by the BC coating effect across the Northern
13 Hemisphere, by combining model simulations with in situ observations of BC and OC
14 concentrations in snow.

15 **2 Methods**

16 **2.1 Modeling**

17 **2.1.1 Optical parameter calculations for coated BC**

18 Figure 1a and 1c shows schematics of light absorption by externally and internally
19 mixed particles (EMP and IMP, respectively). EMP refers to uncoated BC mixed with
20 other particles, while IMP refers to BC that is assumed to be a core coated by another
21 particle acting as a shell (Kahnert et al., 2012). For a non-absorbing shell, overall light



1 absorption includes contributions from the BC core and enhancement absorption from
2 a lensing effect, while for an absorbing shell, the shell itself also contributes to light
3 absorption.

4 To evaluate the BC coating effect on snow albedo, it is necessary to determine the
5 optical parameters of coated BC. The refractive index (RI) of BC was assumed to be
6 $1.95-0.79i$ following Lack and Cappa (2010), which is consistent with the original
7 SNICAR model (Flanner et al., 2007). Two types of particle shells (non-absorbing and
8 absorbing) were considered. The non-absorbing shell was represented using sulfate,
9 and its RI was assumed to be $1.55-10^{-6}i$ following the atmospheric study of Bond et al.
10 (2006). The absorbing shell was represented using OC, which is a major light-absorbing
11 particle in snow (Wang et al., 2013). The RI of OC varies with wavelength. Here, a
12 fixed mass absorption coefficient (MAC) for OC of $0.3 \text{ m}^2 \text{ g}^{-1}$ at 550 nm, a real RI of
13 1.55, and a particle diameter of 200 nm were assumed, following Lack and Cappa
14 (2010). Based on Mie theory, an imaginary RI value of $-1.36 \times 10^{-2}i$ at 550 nm was
15 calculated. Subsequently, wavelength-dependent imaginary RI values (Figure S1) were
16 derived according to an absorption angstrom exponent (AAE) of -6 (Sun et al., 2007).

17 For a core/shell-structured particle, the core and shell diameters refer to the BC
18 core diameter and the whole particle diameter, respectively. BC diameters are usually
19 in the range of $\sim 50-120$ nm in the atmosphere (Corbin et al., 2018), and are typically
20 larger by ~ 20 nm in snow due to a removal process via wet deposition (Schwarz et al.,
21 2013). Therefore, we assumed the BC diameter in snow was 100 nm. Core and shell



1 diameters, RI, and wavelength were then used in a Mie model to derive optical
2 parameters of the core/shell particle, including single scatter albedo (SSA), asymmetry
3 factor (g), and extinction cross-section (Q_{ext}). The mass extinction coefficient (MEC)
4 of the core/shell particle was calculated based on Q_{ext} and the density, given as 1.8 g
5 cm^{-3} for BC (Bond et al., 2006), 1.2 g cm^{-3} for sulfate, and 1.2 g cm^{-3} for OC (Turpin
6 and Lim, 2001).

7 **2.1.2 Snow albedo calculations**

8 We simulated snow albedo with the SNICAR model (Flanner et al., 2007), which
9 calculates the radiative transfer in snowpack based on the theory of Warren and
10 Wiscombe (1980) and a two-stream multilayer radiative approximation (Toon et al.,
11 1989). Here, we summarize only the model features in SNICAR that are crucial to our
12 study. SNICAR allows for a vertical multilayer distribution of snow properties, LAPs,
13 and heating throughout the snowpack column. Input optical parameters (MEC, SSA,
14 and g) of snow grains and BC were calculated off-line using Mie theory. SNICAR
15 provides albedo changes from uncoated and sulfate-coated BC on snow, as well as dust
16 particles and volcanic ash (for further details, see Flanner et al., 2007).

17 For SNICAR snow albedo simulations of uncoated BC, concentrations of both BC
18 and other particles were input directly. For coated BC, optical parameters (MEC, SSA,
19 and g) of IMP (calculated above) were first archived as lookup tables within SNICAR,
20 and then the concentration of IMP was input.

21 **2.2 Calculation of broadband snow albedo**



1 The spectral albedo (α_λ) was integrated over the solar spectrum ($\lambda = 300\text{--}2500$ nm)
2 and weighted by the incoming solar irradiance (S_λ) to calculate broadband snow albedo
3 ($\alpha_{\text{integrated}}$):

$$4 \quad \alpha_{\text{integrated}} = \frac{\int \alpha_\lambda S_\lambda d\lambda}{\int S_\lambda d\lambda} \quad (1)$$

5 The incoming solar irradiance was a typical surface solar spectrum for mid-high
6 latitudes from January to May, calculated with the Santa Barbara DISORT Atmospheric
7 Radiative Transfer (SBDART) model (Pu et al., 2019), which is one of the most widely
8 used models for radiative transfer simulations (for further details, see Ricchiazzi et al.
9 1998).

10 2.3 Parameterizations

11 In the original SNICAR model, the BC coating effect is simply parameterized with
12 an absorption enhancement of ~ 1.5 (Flanner et al., 2007). However, the effect of BC
13 coating on snow albedo is widely variable and dependent on BC concentration,
14 core/shell ratio, snow grain size, and the type of particle shell (see Section 3.3). In view
15 of this complexity, more explicit parameterizations were developed in this study:

$$16 \quad E_{\alpha, \text{integrated}} = \frac{\alpha_{\text{int, integrated}}}{\alpha_{\text{ext, integrated}}} \quad (2)$$

17 where $\alpha_{\text{ext, integrated}}$ and $\alpha_{\text{int, integrated}}$ are broadband snow albedos for EMP
18 and IMP, respectively. Following a previous empirical formulation (Hadley and
19 Kirchstetter, 2012), $E_{\alpha, \text{integrated}}$ was parameterized as

$$20 \quad E_{\alpha, \text{integrated, para}} = a_0 \times (C_{BC})^{a_1} + a_2 \quad (3)$$

$$21 \quad a_1 = b_0 \times (\log_{10}(R_{ef}/50))^{b_1} \quad (4)$$



1 where $E_{\alpha, \text{integrated, para}}$ is the parameterized $E_{\alpha, \text{integrated}}$, C_{BC} is the BC
2 concentration, and R_{ef} represents the snow grain radius. The terms a_0 , a_1 , a_2 , b_0 ,
3 and b_1 are the empirical coefficients and dependent on the core/shell ratio and the type
4 of particle shell. To enhance the precision, parameterizations were divided into two
5 groups: the first to account for relatively clean snow (with BC concentrations $< 200 \text{ ng}$
6 g^{-1}) and the second for relatively polluted snow ($200 \text{ ng g}^{-1} < \text{BC concentrations} < 1000$
7 ng g^{-1}).

8 **2.4 Calculation of in situ snow albedo and radiative forcing**

9 In situ broadband clear-sky ($\alpha_{\text{integrated}}^{\text{clear, in-situ}}$) and cloudy-sky ($\alpha_{\text{integrated}}^{\text{cloudy, in-situ}}$) albedos
10 were calculated separately based on in situ snow-LAP parameters and SBDART
11 simulated clear-sky and cloudy-sky incoming solar irradiance by assuming a semi-
12 infinite snowpack. The in situ all-sky albedo ($\alpha_{\text{integrated}}^{\text{all-sky, in-situ}}$) was then calculated using
13 weighted clear-sky and cloudy-sky albedos depending on cloud fraction (CF), given as:

$$14 \quad \alpha_{\text{integrated}}^{\text{all-sky, in-situ}} = \text{CF} \times \alpha_{\text{integrated}}^{\text{cloudy, in-situ}} + (1 - \text{CF}) \times \alpha_{\text{integrated}}^{\text{clear, in-situ}} \quad (5)$$

15 In situ radiative forcing by LAPs was calculated by multiplying the derived
16 broadband albedo reduction by the downward shortwave flux at the snow surface (Dang
17 et al., 2017). Figure S2 shows the spatial distributions of solar flux and cloud fraction,
18 which were obtained from the Clouds and the Earth's Radiant Energy System (CERES)
19 (<https://ceres.larc.nasa.gov/products.php?product=SYN1deg>).

20 **3 Results and discussion**

21 **3.1 Impact on particle light absorption**



1 Figure 1b and 1d shows light absorption ratios (light absorption enhancement, E_{abs})
2 for IMP versus EMP. Based on Bond et al. (2006), we show the most common core/shell
3 ratios (the ratio of the diameter of the whole particle to the BC core) of 1.2, 1.5, 2.0,
4 and 2.5 in real environments to represent the thickness of shells, and we used detailed
5 core/shell ratios from 1.1 to 3.0 (in intervals of 0.1) for parameterizations (see Section
6 3.5). E_{abs} varies with the wavelength and increases with core/shell ratio, in contrast to
7 the default E_{abs} value used in the original SNICAR model, which remains constant. For
8 a non-absorbing shell, the light absorption of IMP is larger than EMP across all
9 wavelengths (300–1400 nm). For an absorbing shell, E_{abs} is similar to the non-absorbing
10 shell in NIR, but becomes smaller in visible (VIS) light and ultra-violet (UV), which
11 implies the absorbing shell reduces whole-particle light absorption and contributes
12 negatively to E_{abs} . A plausible explanation is that the shell absorbs incident photons,
13 causing fewer to reach the core. In such a case, the additional photons absorbed by the
14 shell are fewer than the reduced number of photons absorbed by the lensing effect and
15 the BC core. Furthermore, the absorbing shell reduces E_{abs} to <1 in UV at high
16 core/shell ratios, implying that the lensing effect absorption at those wavelengths
17 cannot recover the BC core absorption reduction, resulting in fewer photons reaching
18 the core.

19 **3.2 Impact on spectral snow single-scattering properties and albedos**

20 In real snowpack, BC can effectively enhance snow single-scattering co-albedo
21 ($1-\omega$), but its effect on other snow optical parameters, such as the asymmetry factor



1 and extinction efficiency, is negligible (He et al., 2017). Therefore, we focus our
2 discussion on coating-induced enhancement of snow single-scattering co-albedo ($E_{1-\omega}$),
3 snow albedo (E_α), and snow albedo reduction ($E_{\Delta\alpha}$).

4 The coating effect has a clear influence on $E_{1-\omega}$ and E_α in UV and VIS, but affects
5 $E_{\Delta\alpha}$ across all wavelengths (Figure 2). The core/shell ratio makes a positive contribution
6 to $E_{1-\omega}$ and $E_{\Delta\alpha}$, and a negative contribution to E_α . The BC concentration makes a
7 positive contribution to $E_{1-\omega}$ and a negative contribution to $E_{\Delta\alpha}$ and E_α . For a given BC
8 concentration and core/shell ratio, $E_{1-\omega}$ and $E_{\Delta\alpha}$ decrease, and E_α increases, with longer
9 wavelength from UV to VIS. In addition, the absorbing shell shows a negative influence
10 for $E_{1-\omega}$ and $E_{\Delta\alpha}$, but positive for E_α compared with a non-absorbing shell, particularly
11 under UV. Moreover, for an absorbing shell, $E_{1-\omega}$ and $E_{\Delta\alpha}$ are <1 , and E_α is >1 at
12 approximately <350 nm in the case of high core/shell ratios because of lower light
13 absorption by IMP than EMP at those wavelengths.

14 **3.3 Impact on broadband snow single-scattering properties and albedos**

15 Compared with spectral optical properties, our broadband results have wider
16 implications for the research community. Core/shell ratios dominate variations in
17 spectrally weighted $E_{1-\omega, \text{integrated}}$, $E_{\alpha, \text{integrated}}$, and $E_{\Delta\alpha, \text{integrated}}$ (Figure 3). Snow grain size
18 and BC concentration show a negative contribution to $E_{\alpha, \text{integrated}}$, but barely affect $E_{\Delta\alpha, \text{integrated}}$.
19 However, the type of particle shell has a significant impact on $E_{1-\omega, \text{integrated}}$, $E_{\alpha, \text{integrated}}$,
20 $E_{\Delta\alpha, \text{integrated}}$, and $E_{\Delta\alpha, \text{integrated}}$. Compared with $E_{1-\omega, \text{integrated}}$ and $E_{\alpha, \text{integrated}}$, $E_{\Delta\alpha, \text{integrated}}$ has a
21 more direct influence on radiative forcing and climate change. $E_{\Delta\alpha, \text{integrated}}$ largely falls



1 within a range of 1.11 to ~1.80 for a non-absorbing shell, which exceeds the values for
2 an absorbing shell (1.10 to ~1.33) by a factor of 1.0–1.35 (with BC concentrations
3 within 1000 ng g^{-1} , a snow grain radius of 100–500 μm , and core/shell ratios from 1.2
4 to 2.5). In contrast, the $E_{\Delta\alpha, \text{integrated}}$ from the original SNICAR model only shows a small
5 variation of 1.23–1.31. This is similar to a non-absorbing shell with a core/shell ratio
6 of ~1.5, which implies the original SNICAR model only reflects a coating effect on
7 snow albedo reduction at an intermediate core/shell ratio.

8 **3.4 Uncertainties**

9 Although the imaginary RI value of OC has been theoretically calculated (Section
10 2.1), we note that in real snowpack there is large uncertainty because the types and
11 optical properties of OC varies spatially and temporally due to different emission
12 sources and photochemical reactions in the atmosphere (e.g. Lack and Cappa, 2010).
13 To address this issue, we tested the degree of influence of imaginary RI on $E_{\alpha, \text{integrated}}$,
14 and $E_{\Delta\alpha, \text{integrated}}$ values by increasing and decreasing the calculated imaginary RI by 50%
15 (Figure S1), which studies have shown to be plausible (e.g., Lack et al., 2012). We find
16 imaginary RI uncertainty to be $\pm 1\%$ for $E_{\alpha, \text{integrated}}$ and $\pm 5\%$ for $E_{\Delta\alpha, \text{integrated}}$.

17 In addition, observations show large variation in the size distribution of
18 atmospheric and snow BC particles (Schwarz et al., 2013), which can affect snow
19 optical properties and albedo (He et al., 2018). Therefore, we examined the effects of
20 BC particle size on $E_{\alpha, \text{integrated}}$ and $E_{\Delta\alpha, \text{integrated}}$ with two additional BC diameters of 50
21 nm and 150 nm, which are within observed size ranges (Schwarz et al., 2013) and are



1 comparable to BC particle sizes used in other studies (e.g. He et al., 2018). We find the
2 uncertainty attributed to BC diameter is $\pm 1\%$ for $E_{\alpha, \text{integrated}}$ and $\pm 13\%$ for $E_{\Delta\alpha, \text{integrated}}$.
3 Overall, the total uncertainty related to imaginary RI and BC diameter is $\pm 1.4\%$ for $E_{\alpha, \text{integrated}}$
4 and $\pm 13.9\%$ for $E_{\Delta\alpha, \text{integrated}}$.

5 **3.5 Parameterizations of the coating effect**

6 Figure 4 compares parameterized $E_{\alpha, \text{integrated, para}}$ with SNICAR-modeled $E_{\alpha, \text{integrated}}$,
7 and Tables S1 and S2 list the empirical coefficients (see Section 2.3) derived from
8 nonlinear regression processes. $E_{\alpha, \text{integrated, para}}$ and $E_{\alpha, \text{integrated}}$ show a strong correlation,
9 with $R^2 = 0.988$ (0.986) for a non-absorbing shell and $R^2 = 0.987$ (0.986) for an
10 absorbing shell in relatively clean (polluted) snow, and root mean squared errors of
11 1.81×10^{-3} (4.70×10^{-3}) and 1.41×10^{-3} (3.76×10^{-3}), respectively. Biases for $E_{\alpha, \text{integrated, para}}$
12 are smallest for intermediate BC concentrations and snow grain radius, but
13 become larger at extremely low or high values, due mainly to processes within the
14 nonlinear regression method. Overall, the $E_{\alpha, \text{integrated}}$ can be well reproduced by $E_{\alpha, \text{integrated, para}}$
15 for both a non-absorbing and absorbing shell under the conditions of both
16 relatively clean and polluted snow.

17 Therefore, other studies can estimate the coating effect of BC on snow albedos
18 and radiative forcing very conveniently by combining the original SNICAR or other
19 snow radiative forcing model with our new parameterizations, which can reduce snow
20 albedo simulation bias. For example, Wang et al. (2017) compared observations and
21 model simulations of snow albedo reduction in northern China. They found simulated



1 results overestimated snow albedo by ~ 0.06 in polluted snow, despite considering the
2 effects of all LAP types (BC, OC, and dust), snow grain type, and snow depth. However,
3 if the coating effect is taken into account and the new parameterizations are applied
4 (according to their measured LAPs and snow parameters), the difference between
5 simulation and observation is reduced to ~ 0.02 , thereby improving the simulation.
6 Furthermore, although most global climate models (GCMs) account for internal mixing
7 of atmospheric BC, they barely consider the coating effect for BC in snow (Bond et al.,
8 2013). In addition, different GCMs apply different types of snow radiative transfer
9 models, which means that one physical mechanism responsible for the BC coating
10 effect in snow cannot be suitable for all GCMs. In this case our parameterizations are
11 particularly helpful, as they are easily used in any GCM and improve understanding of
12 how BC in snow influences local hydrological cycles and global climate.

13 **3.6 Measurement-based estimate of coating effect**

14 To evaluate the coating effect of BC on both snow albedo and radiative forcing in
15 real snowpack, we collected in situ measurements of BC and OC concentrations in
16 snow (Figure 5) during field campaigns in the Arctic in spring 2007–2009 (Doherty et
17 al., 2010), North America in January–March 2013 (Doherty et al., 2014), northern
18 China in January–February 2010 and 2012 (Ye et al., 2012; Wang et al., 2013), and the
19 Tibetan Plateau in spring 2010 and 2012 (Wang et al., 2013; Li et al., 2017, 2018; Pu
20 et al., 2017; Zhang et al., 2017, 2018). Measurements are separated into four
21 geographical regions (Figure 5c): the Arctic, North America (NA), northern China (NC),



1 and the Tibetan Plateau (TP). An absorbing shell of OC was assumed in measured
2 snowpack, which is plausible because previous studies have found that OC is the
3 dominant coating in the atmosphere (e.g., Cappa et al., 2012). The OC/BC mass ratio
4 is generally from 1 to 10, with the corresponding core/shell ratio from 1.3 to 2.5 (Figure
5 5b). The average core/shell ratio was highest (2.45) in the TP, followed by 1.92 and
6 1.81 in the Arctic and NC, respectively, and lowest (1.31) in NA (Figure 5d). These
7 results reveal the BC coating effect had a larger impact on snow albedo in the TP than
8 in other regions.

9 Figure 6 presents the coating effect on snow albedo reduction and radiative forcing
10 based on measured BC in real snowpack, and Figures S3–S5 show spatial distributions
11 and statistics. For fresh snow, we find that IMP results in greater snow albedo reductions
12 compared with EMP by factors of 1.27, 1.19, 1.13, and 1.23 in the TP, NC, NA, and the
13 Arctic, respectively (Figure 6a and b). Correspondingly, we find that IMP leads
14 radiative forcing by 1.27, 1.20, 1.14, and 1.22 for these same regions. The highest
15 (lowest) enhancement was found in the TP (NA), which corresponds to the highest
16 (lowest) OC/BC mass ratio and core/shell ratio in the TP (NA). For old snow, the
17 enhancement of snow albedo reductions due to the BC coating effect are 1.24, 1.15,
18 1.13, and 1.23 in TP, NC, NA, and the Arctic, respectively. The corresponding radiative
19 forcing reductions are 1.24, 1.16, 1.14, and 1.22. The enhancement shows a slight
20 decrease with snowpack aging, which is consistent with the results in Figure 3. Of note,
21 we found the contribution of coating effect to light absorption has exceeded dust over



1 most areas of northern China after comparing with previous studies of dust in snow
2 (Wang et al., 2013, 2017; Pu et al., 2017), which further demonstrated the critical role
3 of BC coatings in snow albedo evaluation.

4 In contrast to previous studies, we note that enhanced light absorption in snow
5 from the BC coating effect should be taken into account, especially in the Arctic and
6 the TP. Arctic sea ice has shown a sharp decline in recent decades (Ding et al., 2019),
7 and climate models predict a continued decreasing trend (Liu et al., 2020) that is likely
8 to perturb the Earth system and influence human activities (Meier et al., 2014). Multi-
9 model ensemble simulations indicate that greenhouse gases cannot fully explain this
10 decline, and recent studies have proposed that BC deposition in snow and sea ice is an
11 important additional contributor (e.g., Ramanathan and Carmichael, 2008).
12 Furthermore, the TP holds the largest ice mass outside polar regions, and acts as a water
13 ‘storage tower’ for more than 1 billion people in South and East Asia. Tibetan glaciers
14 have rapidly retreated over the last 30 years (Yao et al., 2012), raising the possibility
15 that many glaciers and their fresh water supplies could disappear by the middle of the
16 21st century. Observed evidence suggests that BC deposition is a significant
17 contributing factor to this retreat (Xu et al., 2009), but quantitatively modeling the effect
18 of BC on glacier dynamics is a challenge, partly because of incomplete radiative
19 transfer mechanisms within models. Due to the significant contribution of BC to
20 retreating Arctic sea ice and Tibetan glaciers, and the strong enhancement of light
21 absorption by coated BC, the coating effect must now be considered in climate models



1 that are designed to accurately reconstruct both the historical record and future change.

2 **4 Conclusions**

3 This study evaluated the effect of BC coating on snow albedo and radiative forcing
4 by combining core/shell Mie theory and the snow-albedo model SNICAR. We found that
5 the coating effect reduces snow albedo by a factor of 1.11–1.80 for a non-absorbing
6 shell and 1.10–1.33 for an absorbing shell, when BC concentrations are within 1000 ng
7 g^{-1} , the snow grain radius is 100–500 μm , and the core/shell ratio is 1.2–2.5. The
8 core/shell ratio plays a dominant role in reducing snow albedo. Furthermore, an
9 absorbing shell causes a smaller snow albedo reduction than a non-absorbing shell
10 because of a lensing effect, whereby the absorbing shell reduces photon absorbance in
11 the BC core. Our results can effectively account for the complex enhancement of snow
12 albedo reduction due to coating effect in real environments.

13 Parameterizations for the coating effect are further developed for use in snow
14 albedo and climate models. Parameterized and simulated results show strong
15 correlations for both clean and polluted snowpack. The root mean squared error of
16 parameterized $E_{\alpha, \text{integrated, para}}$ is low (1.41×10^{-3}). A list of empirical coefficients for
17 parameterizations is provided for most seasonal snowpack field cases, with BC
18 concentrations within 1000 ng g^{-1} , snow grain sizes from 100–1000 μm , and core/shell
19 ratios from 1.1 to 3.0. We demonstrate that parameterizations can reduce simulation
20 bias for local experiments in snow albedo models and, more importantly, can be applied
21 to GCMs to improve our understanding of how BC in snow affects local hydrological



1 cycles and global climate.

2 Based on a comprehensive set of field measurements across the Northern

3 Hemisphere, the BC coating effect in real snowpack was evaluated by assuming the

4 presence of an absorbing OC shell. The enhancement of snow albedo reduction was

5 1.133–1.273 and enhancement of radiative forcing was 1.135–1.274, which exceeds the

6 contribution of dust to snow light absorption over most areas of northern China. Of

7 note, the greatest enhancements were detected on the Tibetan Plateau and in the Arctic,

8 which will likely contribute to further Arctic sea ice and Tibetan glacier retreat. Our

9 findings indicate that the coating effect must be considered in future climate models, in

10 particular to more accurately evaluate the climate of the Tibetan Plateau and the Arctic.



1 **Conflict of interest**

2 The authors declare that they have no conflict of interest.

3 **Acknowledgments**

4 This research was supported jointly by the National Key R&D Program of China
5 (2019YFA0606801), the National Natural Science Foundation of China (41975157 and
6 41775144), and the China Postdoctoral Science Foundation (2020M673530).

7 **Author contributions**

8 X Wang and W Pu invited the project. W Pu and X Wang designed the study. W
9 Pu wrote the paper with contributions from all co-authors. TL Shi processed and
10 analyzed the data.



1 References

- 2 Aquila, V., Hendricks, J., Lauer, A., Riemer, N., Vogel, H., Baumgardner, D., Minikin,
3 A., Petzold, A., Schwarz, J., and Spackman, J.: MADE-in: A new aerosol
4 microphysics submodel for global simulation of insoluble particles and their
5 mixing state, *Geosci. Model Dev.*, 4, 325-355, 2011.
- 6 Bond, T. C., Habib, G., and Bergstrom, R. W.: Limitations in the enhancement of
7 visible light absorption due to mixing state, *J. Geophys. Res.-Atmos.*, 111, D20,
8 2006.
- 9 Bond, T. C., Doherty, S. J., Fahey, D. W., Forster, P. M., Berntsen, T., DeAngelo, B.
10 J., Flanner, M. G., Ghan, S., Karcher, B., Koch, D., Kinne, S., Kondo, Y., Quinn,
11 P. K., Sarofim, M. C., Schultz, M. G., Schulz, M., Venkataraman, C., Zhang, H.,
12 Zhang, S., Bellouin, N., Guttikunda, S. K., Hopke, P. K., Jacobson, M. Z., Kaiser,
13 J. W., Klimont, Z., Lohmann, U., Schwarz, J. P., Shindell, D., Storelvmo, T.,
14 Warren, S. G., and Zender, C. S.: Bounding the role of black carbon in the climate
15 system: A scientific assessment, *J. Geophys. Res.-Atmos.*, 118, 5380-5552, 2013.
- 16 Cappa, C. D., Onasch, T. B., Massoli, P., Worsnop, D. R., Bates, T. S., Cross, E. S.,
17 Davidovits, P., Hakala, J., Hayden, K. L., Jobson, B. T., Kolesar, K. R., Lack, D.
18 A., Lerner, B. M., Li, S. M., Mellon, D., Nuaaman, I., Olfert, J. S., Petaja, T.,
19 Quinn, P. K., Song, C., Subramanian, R., Williams, E. J., and Zaveri, R. A.:
20 Radiative Absorption Enhancements Due to the Mixing State of Atmospheric
21 Black Carbon, *Science*, 337, 1078-1081, 2012.
- 22 Cohen, J., and Rind, D.: The effect of snow cover on the climate, *J. Climate*, 4, 689-
23 706, 1991.
- 24 Corbin, J. C., Pieber, S. M., Czech, H., Zanatta, M., Jakobi, G., Massabò, D., Orasche,
25 J., El Haddad, I., Mensah, A. A., and Stengel, B.: Brown and black carbon emitted
26 by a marine engine operated on heavy fuel oil and distillate fuels: optical
27 properties, size distributions, and emission factors, *J. Geophys. Res.-Atmos.*, 123,
28 6175-6195, 2018.
- 29 Dang, C., Fu, Q., and Warren, S. G.: Effect of Snow Grain Shape on Snow Albedo, *J.*
30 *Atmos. Sci.*, 73, 3573-3583, 2016.
- 31 Dang, C., Warren, S. G., Fu, Q., Doherty, S. J., and Sturm, M.: Measurements of light-
32 absorbing particles in snow across the Arctic, North America, and China: effects
33 on surface albedo, *J. Geophys. Res.-Atmos.*, 122, 10149-10168, 2017.
- 34 Ding, Q., Schweiger, A., L'Heureux, M., Steig, E. J., Battisti, D. S., Johnson, N. C.,
35 Blanchard-Wrigglesworth, E., Po-Chedley, S., Zhang, Q., and Harnos, K.:
36 Fingerprints of internal drivers of Arctic sea ice loss in observations and model
37 simulations, *Nat. Geosci.*, 12, 28-33, 2019.
- 38 Doherty, S. J., Warren, S. G., Grenfell, T. C., Clarke, A. D., and Brandt, R. E.: Light-
39 absorbing impurities in Arctic snow, *Atmos. Chem. Phys.*, 10, 11647-11680, 2010.
- 40 Doherty, S. J., Dang, C., Hegg, D. A., Zhang, R., and Warren, S. G.: Black carbon and
41 other light-absorbing particles in snow of central North America, *J. Geophys.*



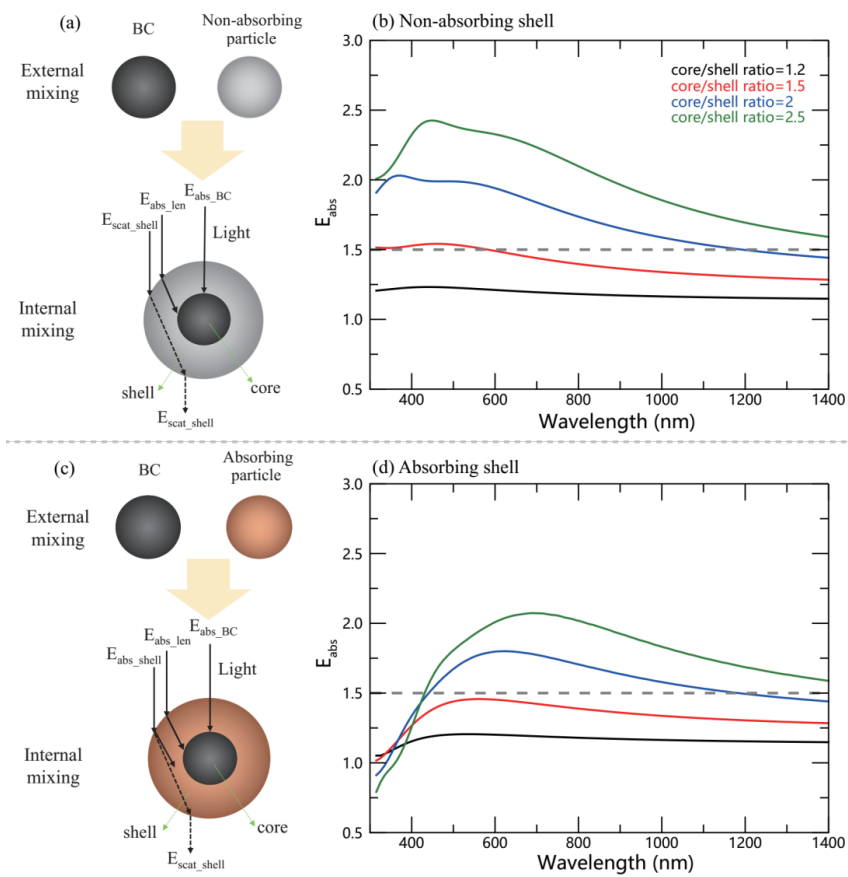
- 1 Res.-Atmos., 119, 12807-12831, 2014.
- 2 Flanner, M. G., Zender, C. S., Randerson, J. T., and Rasch, P. J.: Present-day climate
3 forcing and response from black carbon in snow, *J. Geophys. Res.*, 112, D11, 2007.
- 4 Hadley, O. L., and Kirchstetter, T. W.: Black-carbon reduction of snow albedo, *Nat.*
5 *Clim. Change*, 2, 437-440, 2012.
- 6 He, C., Takano, Y., Liou, K. N., Yang, P., Li, Q., Chen, F., He, C., Takano, Y., Liou,
7 K. N., and Yang, P.: Impact of Snow Grain Shape and Black Carbon-Snow
8 Internal Mixing on Snow Optical Properties: Parameterizations for Climate
9 Models, *J. Climate*, 30, 10019-10036, 2017.
- 10 He, C. L., Liou, K. N., and Takano, Y.: Resolving Size Distribution of Black Carbon
11 Internally Mixed With Snow: Impact on Snow Optical Properties and Albedo,
12 *Geophys. Res. Lett.*, 45, 2697-2705, 2018.
- 13 Jacobson, M. Z.: Strong radiative heating due to the mixing state of black carbon in
14 atmospheric aerosols, *Nature*, 409, 695-697, 2001.
- 15 Kahnert, M., Nousiainen, T., Lindqvist, H., and Ebert, M.: Optical properties of light
16 absorbing carbon aggregates mixed with sulfate: assessment of different model
17 geometries for climate forcing calculations, *Opt. Express*, 20, 10042-10058, 2012.
- 18 Lack, D. A., and Cappa, C. D.: Impact of brown and clear carbon on light absorption
19 enhancement, single scatter albedo and absorption wavelength dependence of
20 black carbon, *Atmos. Chem. Phys.*, 10, 4207-4220, 2010.
- 21 Lack, D. A., Langridge, J. M., Bahreini, R., Cappa, C. D., Middlebrook, A. M., and
22 Schwarz, J. P.: Brown carbon and internal mixing in biomass burning particles,
23 *PNAS*, 109, 14802-14807, 2012.
- 24 Li, X., Kang, S., He, X., Qu, B., Tripathee, L., Jing, Z., Paudyal, R., Li, Y., Zhang, Y.,
25 and Yan, F.: Light-absorbing impurities accelerate glacier melt in the Central
26 Tibetan Plateau, *Sci. Total Environ.*, 587, 482-490, 2017.
- 27 Li, X., Kang, S., Zhang, G., Qu, B., Tripathee, L., Paudyal, R., Jing, Z., Zhang, Y., Yan,
28 F., and Li, G.: Light-absorbing impurities in a southern Tibetan Plateau glacier:
29 Variations and potential impact on snow albedo and radiative forcing, *Atmos. Res.*,
30 200, 77-87, 2018.
- 31 Liu, D. T., Whitehead, J., Alfarra, M. R., Reyes-Villegas, E., Spracklen, D. V.,
32 Reddington, C. L., Kong, S. F., Williams, P. I., Ting, Y. C., Haslett, S., Taylor, J.
33 W., Flynn, M. J., Morgan, W. T., McFiggans, G., Coe, H., and Allan, J. D.: Black-
34 carbon absorption enhancement in the atmosphere determined by particle mixing
35 state, *Nat. Geosci.*, 10, 184-U132, 2017.
- 36 Liu, J., Wu, D., Liu, G., Mao, R., Chen, S., Ji, M., Fu, P., Sun, Y., Pan, X., and Jin, H.:
37 Impact of Arctic amplification on declining spring dust events in East Asia, *Clim.*
38 *Dyn.*, 54, 1913-1935, 2020.
- 39 Matsui, H., Hamilton, D. S., and Mahowald, N. M.: Black carbon radiative effects
40 highly sensitive to emitted particle size when resolving mixing-state diversity, *Nat.*
41 *Commun.*, 9, 1-11, 2018.
- 42 Meier, W. N., Hovelsrud, G. K., Van Oort, B. E., Key, J. R., Kovacs, K. M., Michel,



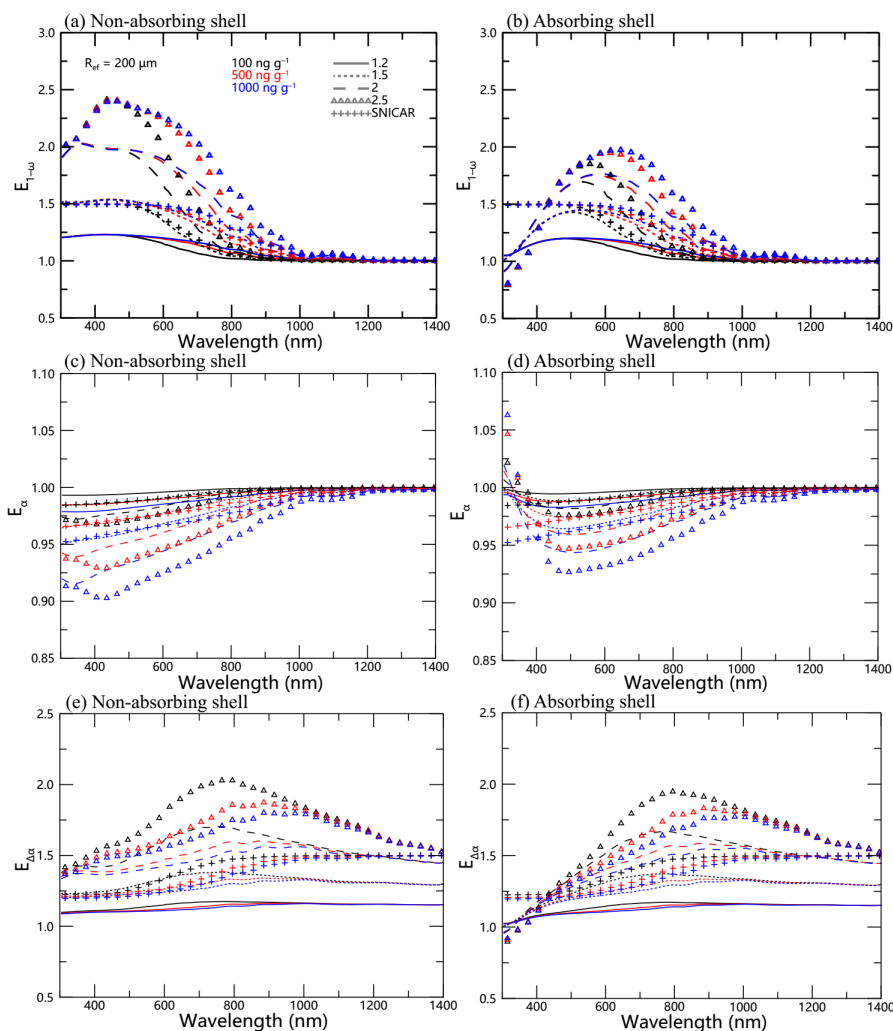
- 1 C., Haas, C., Granskog, M. A., Gerland, S., and Perovich, D. K.: Arctic sea ice in
2 transformation: A review of recent observed changes and impacts on biology and
3 human activity, *Rev. Geophys.*, 52, 185-217, 2014.
- 4 Moffet, R. C., and Prather, K. A.: In-situ measurements of the mixing state and optical
5 properties of soot with implications for radiative forcing estimates, *PNAS*, 106,
6 11872-11877, 2009.
- 7 Moteki, N., Kondo, Y., Miyazaki, Y., Takegawa, N., Komazaki, Y., Kurata, G., Shirai,
8 T., Blake, D. R., Miyakawa, T., and Koike, M.: Evolution of mixing state of black
9 carbon particles: Aircraft measurements over the western Pacific in March 2004,
10 *Geophys. Res. Lett.*, 34, L11803, 2007.
- 11 Peng, J. F., Hu, M., Guo, S., Du, Z. F., Zheng, J., Shang, D. J., Zamora, M. L., Zeng,
12 L. M., Shao, M., Wu, Y. S., Zheng, J., Wang, Y., Glen, C. R., Collins, D. R.,
13 Molina, M. J., and Zhang, R. Y.: Markedly enhanced absorption and direct
14 radiative forcing of black carbon under polluted urban environments, *PNAS*, 113,
15 4266-4271, 2016.
- 16 Pu, W., Wang, X., Wei, H., Zhou, Y., Shi, J., Hu, Z., Jin, H., and Chen, Q.: Properties
17 of black carbon and other insoluble light-absorbing particles in seasonal snow of
18 northwestern China, *The Cryosphere*, 11, 1213-1233, 2017.
- 19 Pu, W., Cui, J. C., Shi, T. L., Zhang, X. L., He, C. L., and Wang, X.: The remote sensing
20 of radiative forcing by light-absorbing particles (LAPs) in seasonal snow over
21 northeastern China, *Atmos. Chem. Phys.*, 19, 9949-9968, 2019.
- 22 Qian, Y., Gustafson, W. I., Leung, L. R., and Ghan, S. J.: Effects of soot-induced snow
23 albedo change on snowpack and hydrological cycle in western United States based
24 on Weather Research and Forecasting chemistry and regional climate simulations,
25 *J. Geophys. Res.-Atmos.*, 114, D3, 2009.
- 26 Ramanathan, V., and Carmichael, G.: Global and regional climate changes due to black
27 carbon, *Nat. Geosci.*, 1, 221-227, 2008.
- 28 Ricchiuzzi, P., Yang, S., Gautier, C., and Sowle, D.: SBDART: A research and teaching
29 software tool for plane-parallel radiative transfer in the Earth's atmosphere, *Bull.*
30 *Amer. Meteor. Soc.*, 79, 2101-2114, 1998.
- 31 Schwarz, J. P., Gao, R. S., Perring, A. E., Spackman, J. R., and Fahey, D. W.: Black
32 carbon aerosol size in snow, *Sci. Rep.*, 3, 1356, 2013.
- 33 Sun, H. L., Biedermann, L., and Bond, T. C.: Color of brown carbon: A model for
34 ultraviolet and visible light absorption by organic carbon aerosol, *Geophys. Res.*
35 *Lett.*, 34, L17813, 2007.
- 36 Toon, O. B., McKay, C. P., Ackerman, T. P., and Santhanam, K.: Rapid Calculation of
37 Radiative Heating Rates and Photodissociation Rates in Inhomogeneous Multiple-
38 Scattering Atmospheres, *J. Geophys. Res.-Atmos.*, 94, 16287-16301, 1989.
- 39 Turpin, B. J., and Lim, H. J.: Species contributions to PM_{2.5} mass concentrations:
40 Revisiting common assumptions for estimating organic mass, *Aerosol Sci. Tech.*,
41 35, 602-610, 2001.
- 42 Wang, X., Doherty, S. J., and Huang, J.: Black carbon and other light-absorbing



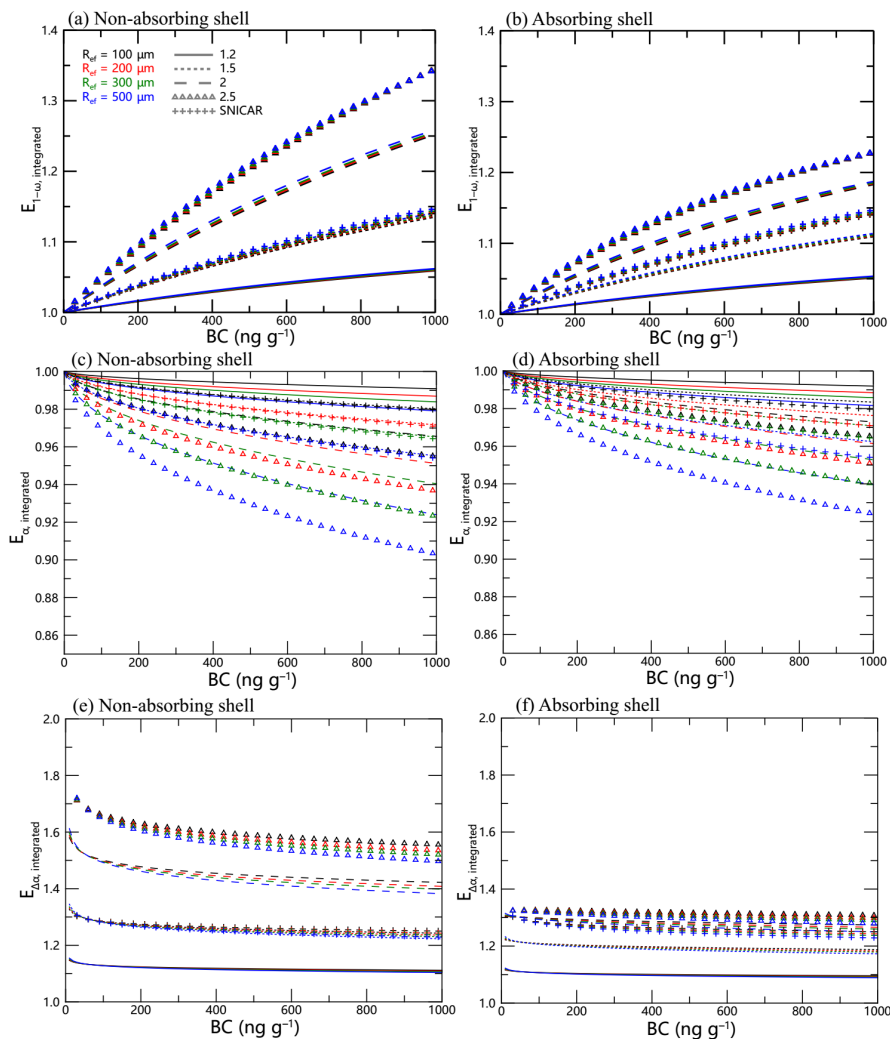
- 1 impurities in snow across Northern China, *J. Geophys. Res.-Atmos.*, 118, 1471-
2 1492, 2013.
- 3 Wang, X., Pu, W., Ren, Y., Zhang, X. L., Zhang, X. Y., Shi, J. S., Jin, H. C., Dai, M.
4 K., and Chen, Q. L.: Observations and model simulations of snow albedo
5 reduction in seasonal snow due to insoluble light-absorbing particles during 2014
6 Chinese survey, *Atmos. Chem. Phys.*, 17, 2279-2296, 2017.
- 7 Warren, S. G., and Wiscombe, W. J.: A Model for the Spectral Albedo of Snow. 2:
8 Snow Containing Atmospheric Aerosols, *J. Atmos. Sci.*, 37, 2734-2745, 1980.
- 9 Xu, B. Q., Cao, J. J., Hansen, J., Yao, T. D., Joswia, D. R., Wang, N. L., Wu, G. J.,
10 Wang, M., Zhao, H. B., Yang, W., Liu, X. Q., and He, J. Q.: Black soot and the
11 survival of Tibetan glaciers, *PNAS*, 106, 22114-22118, 2009.
- 12 Yao, T. D., Thompson, L., Yang, W., Yu, W. S., Gao, Y., Guo, X. J., Yang, X. X.,
13 Duan, K. Q., Zhao, H. B., Xu, B. Q., Pu, J. C., Lu, A. X., Xiang, Y., Kattel, D. B.,
14 and Joswiak, D.: Different glacier status with atmospheric circulations in Tibetan
15 Plateau and surroundings, *Nat. Clim. Change*, 2, 663-667, 2012.
- 16 Ye, H., Zhang, R., Shi, J., Huang, J., Warren, S. G., and Fu, Q.: Black carbon in seasonal
17 snow across northern Xinjiang in northwestern China, *Environ. Res. Lett.*, 7,
18 044002, 2012.
- 19 You, R., Radney, J. G., Zachariah, M. R., and Zangmeister, C. D.: Measured
20 Wavelength-Dependent Absorption Enhancement of Internally Mixed Black
21 Carbon with Absorbing and Nonabsorbing Materials, *Environ. Sci. Technol.*, 50,
22 7982-7990, 2016.
- 23 Zhang, Y., Kang, S., Cong, Z., Schmale, J., Sprenger, M., Li, C., Yang, W., Gao, T.,
24 Sillanpää, M., and Li, X.: Light-absorbing impurities enhance glacier albedo
25 reduction in the southeastern Tibetan Plateau, *J. Geophys. Res.-Atmos.*, 122,
26 6915-6933, 2017.
- 27 Zhang, Y., Kang, S., Sprenger, M., Cong, Z., Gao, T., Li, C., Tao, S., Li, X., Zhong, X.,
28 and Xu, M.: Black carbon and mineral dust in snow cover on the Tibetan Plateau,
29 *The Cryosphere*, 12, 413-431, 2018.



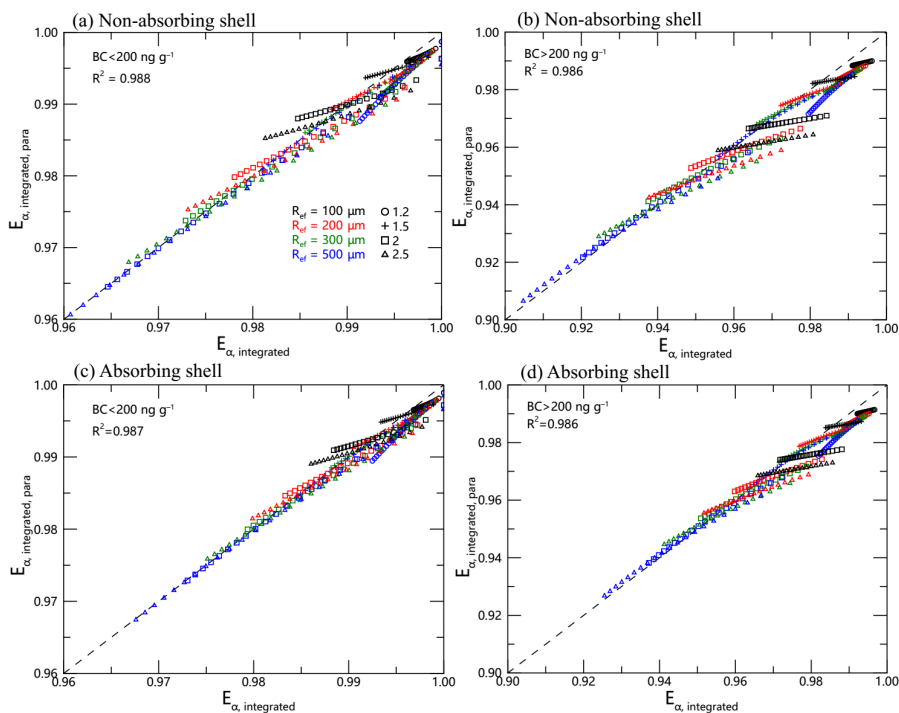
1
 2 **Figure 1.** Schematic diagrams showing the light absorption for an external mixture and
 3 internal mixture of BC, for (a) a non-absorbing particle and (c) an absorbing particle.
 4 Also shown is the enhancement of light absorption from the internal mixture (E_{abs})
 5 compared to the external mixture of BC with (b) non-absorbing and (d) absorbing
 6 particles. The internal mixed particle was assumed to be a core/shell structure with a
 7 black carbon (BC) core.
 8



1
 2 **Figure 2.** Ratios of snow single-scattering co-albedo ($E_{1-\omega}$) from an internal mixed
 3 particle to an external mixed particle as a function of wavelength, with different BC
 4 concentrations and core/shell ratios for (a) a non-absorbing shell, and (b) an absorbing
 5 shell. (c) and (d) Same as (a) and (b), but for snow albedo (E_{α}). (e) and (f) Same as (a)
 6 and (b), but for snow albedo reduction ($E_{\Delta\alpha}$). The snow grain radius was assumed to be
 7 200 nm.
 8

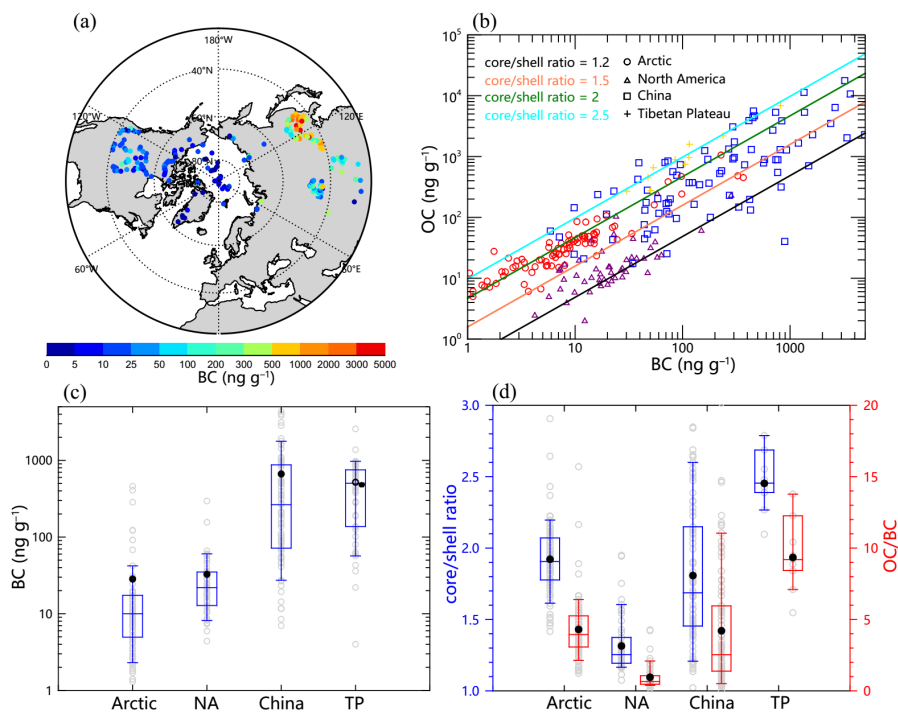


1
 2 **Figure 3.** The spectrally weighted $E_{1-\omega}$ ($E_{1-\omega, \text{integrated}}$) over 300–1400 nm of a typical
 3 surface solar spectrum at mid–high latitude from January to May, for (a) a non-
 4 absorbing shell and (b) an absorbing shell as a function of black carbon (BC)
 5 concentration with different snow grain radii and core/shell ratios. (c) and (d) Same as
 6 (a) and (b), but for broadband snow albedo ($E_{\alpha, \text{integrated}}$). (e) and (f) Same as (a) and (b),
 7 but for broadband snow albedo reduction ($E_{\Delta\alpha, \text{integrated}}$).
 8

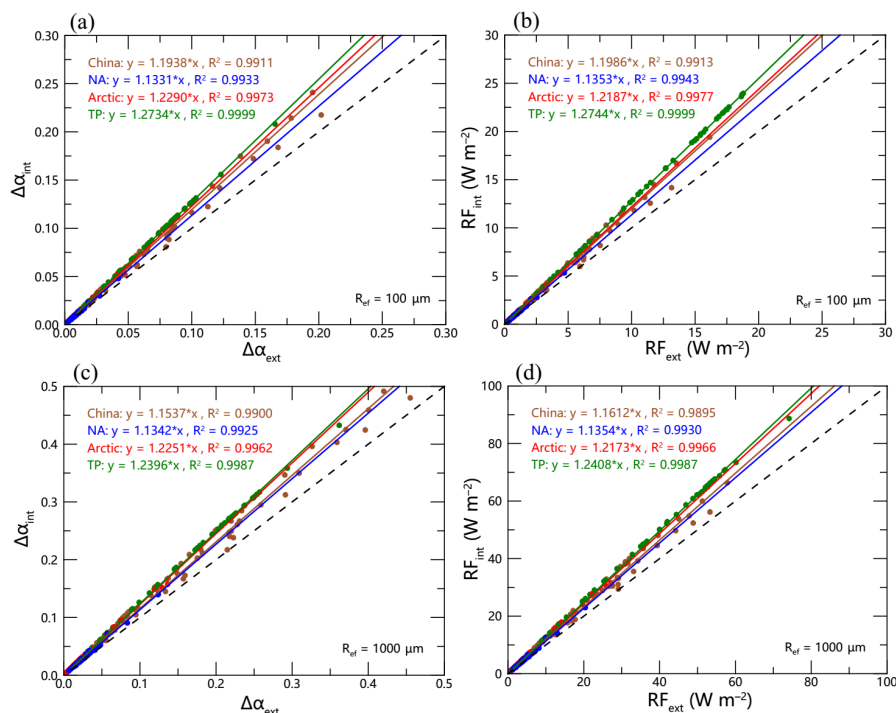


1
2
3
4
5
6

Figure 4. Comparisons of model calculated $E_{\alpha, \text{integrated}}$ and parameterized $E_{\alpha, \text{integrated, para}}$ for (a) relatively clean snow (BC concentration $< 1000 \text{ ng g}^{-1}$), and (b) relatively polluted snow (BC concentration $> 1000 \text{ ng g}^{-1}$) for a non-absorbing shell. (c) and (d) Same as (a) and (b), but for an absorbing shell.



1
2 **Figure 5.** (a) The spatial distribution of measured black carbon (BC) concentrations
3 across the Northern Hemisphere. (b) Comparison of BC and organic carbon (OC)
4 concentrations in: the Arctic, North America (NA), northern China (NC) and the
5 Tibetan Plateau (TP). (c) Statistical plots of BC concentrations in different regions. The
6 boxes denote the 25th and 75th quantiles, the horizontal lines denote the 50th quantiles
7 (medians), solid dots denote averages, and whiskers denote the 10th and 90th quantiles.
8 In situ data is shown as gray circles. (d) Same as (c) but for a core/shell ratio and OC/BC
9 mass ratio, assuming a core/shell structure with a BC core and an absorbing OC shell.
10



1
2 **Figure 6.** Comparisons of (a) the snow albedo reduction and (b) the radiative forcing
3 by an internal mixed particle versus an external mixed particle, based on in situ
4 measurements of fresh snow (assuming a snow grain radius of 100 μm). (c) and (d)
5 Same as (a) and (b), but for old snow and assuming a snow grain radius of 1000 μm .
6